# Nuclear Magnetic Resonance of Hydrogen, Lithium, Fluorine, Boron, and Phosphorus Nuclei

**Garrett Woods**
**University of California, Davis**
**Department of Physics**

**3/12/2010**

**ABSTRACT**

The purpose of this experiment was to accurately measure the g-factors of the nuclei of $^{1}H$ (g= 5.637 ± 0.001), $^{19}F$ (g=5.4297 ± 0.0001), $^{7}Li$ (g=2.11 ± 0.02), $^{11}B$ (g=1.791 ± 0.001), and $^{31}P$ (g=2.268 ± 0.001). These g-factors tend to conform nicely to current accepted values. In addition, the gyromagnetic ratios of these samples were calculated and compared to published values. The $T_2$ relaxation times were also measured from the full width at half max of the NMR signal curves, however, they suffer largely from systematic error and only serve as an upper bound for the measurement.

## INTRODUCTION:

The concept of nuclear magnetic resonance uses several fundamental principles in physics to describe the environment and composition of a sample of atoms. The frequency at which an atom resonates while under the influence of a magnetic field represent a unique signature that can be used to identify that substance. These signatures have many wide ranging applications from medical imaging to physics and chemistry experiments. In this experiment, we measured the gyromagnetic ratios, g-factors, and spin-spin relaxation times of the nuclei of Hydrogen, Fluorine, Lithium, Boron, and Phosphorus.

An atom's nucleus has a magnetic moment described by the vector $\vec{\mu}$ . The magnetic moment is simply a description of which end of the nucleus is the magnetic north pole, and which

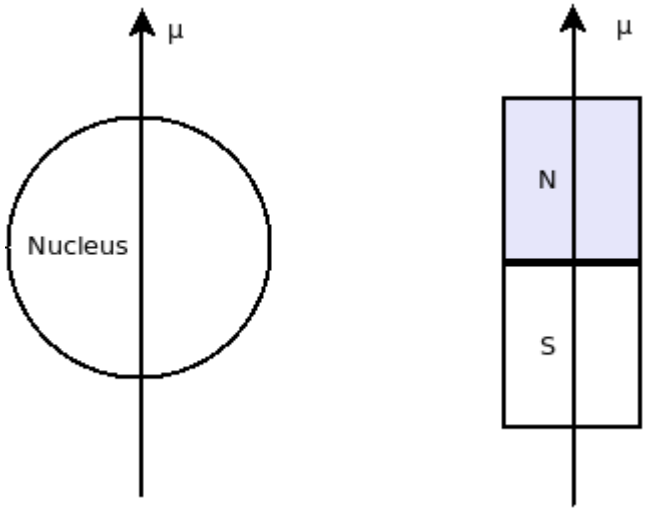


Figure 1: A nuclei's magnetic moment points from south to north just like a bar magnet. Just as a change in an external magnetic field would cause the bar magnet to move and realign itself, a nucleus will also be affected and attempt to align itself with the magnetic field.

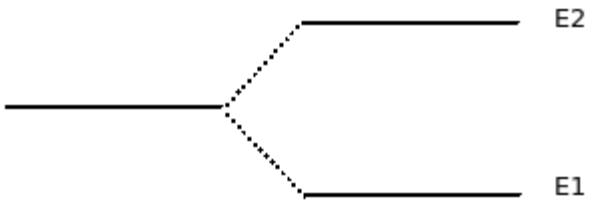


Figure 2: Under the influence of a magnetic field, the energy level of the nucleus is split into two levels, $E_1$ and $E_2$. $E_1$ is occupied by nuclei with their magnetic moments (and spins) aligned parallel with the magnetic field and $E_2$ is occupied by nuclei with their moments aligned perpendicular to the field. After the field is turned on and the energy level split occurs, the nuclei quickly relax to a Boltzmann distribution with the maximum number of nuclei resting in $E_1$.

end is south (see figure 1). In a sample of material containing a large number of atoms, the nuclear moments have a cumulative effect on the macroscopic scale so it is useful to define the magnetization *M* to be

$$\vec{M} = \sum_{i=1}^{n} \vec{\mu}_i \tag{1}$$

which is the magnetic moment of the sample per unit volume. If we were to take this sample and place it in a magnetic field, each nucleus would have an energy described by

$$\vec{E} = \vec{\mu} \cdot \vec{B} \tag{2}$$

where $\vec{B}$ is the vector describing the magnetic field. When this field is applied to a large sample of atoms, it causes the spins of the nuclei to orient themselves either with the magnetic field, or perpendicular to it[1]. In quantum mechanics, this implies that the overall energy level of the sample is split very slightly into two states. A nucleus is in the bottom state when it's magnetic moment is aligned along the direction of the magnetic field and it is in the top state when the moment is aligned perpendicular to the field. These two states are shown in figure 2.

Given these circumstances, the nucleus' magnetic moment experiences a torque $(\vec{\tau})$ equal to

$$\vec{\tau} = \vec{\mu} \times \vec{B} \tag{3}$$

which will cause the moments to precess about the magnetic field vector with a frequency $\omega_o$ (also known as the Larmor frequency) which is defined as

$$\omega_o = \frac{eg}{2m} B \tag{4}$$

where *g* is the g-factor, *m* is the mass of the nucleus, *e* is the elementary charge, and *B* is the magnitude of the magnetic field vector.

As the magnetic field is static in this case, after their initial disturbance the nuclei quickly settle into the lowest energy state possible. This applies to spin ½ fermions so, only a certain number can be in the same energy state at the same time and thus the relaxed distribution is given by the Boltzmann distribution[2]. This simply means that as many nuclei as possible are in $E_1$ (the ground state) and the rest occupy the higher state. Mathematically, the Boltzmann distribution is described by the ratio of the number of particles in the $E_1$ state $(N_1)$ to the number of particles in $E_2$ $(N_2)$ :

$$\frac{N_2}{N_1} = \mathrm{e}^{\frac{\Delta E}{k_b T}} \tag{5}$$

1 For simplicity's sake, the theory presented will focus on a spin ½ nucleus where the energy gets split into two levels. In general however, the number of discrete energy state possibilities is *2S+1* where *S* is the spin of the nucleus. Some of our samples have *S* > ½ and thus have a larger number of energy levels, however the basic idea remains the same.

2 This is also known as “thermal equilibrium”.

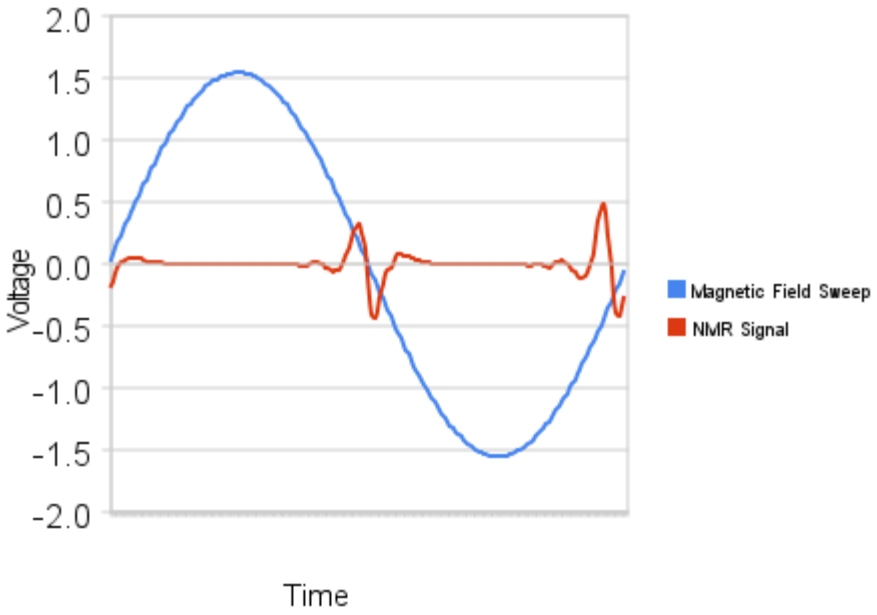


Figure 3: As our magnetic field sweeps slowly up and down, at some point it will match the conditions under which the nucleus will resonate shown here is shown by the intersection of the magnetic field sweep with the NMR curve at approximately zero on the vertical axis.

where $\Delta E$ is the energy difference between $E_1$ and $E_2$, $k_b$ is the Boltzmann constant, and $T$ is the temperature.

As $\vec{M}$ is related to $\vec{\mu}$ by equation (1) the magnetization of the system is related to the difference in populations of the two energy levels such that

$$\vec{M} = (N_1 - N_2)\vec{\mu} \tag{6}$$

This is a static situation; i.e. the magnetic field, and distribution of the nuclei are unchanging with respect to time. So we would expect everything to relax into a static state after a short amount of time[3]. This time is known as the spin-lattice relaxation time, or $T_1$. The average time that a nucleus exists in the upper state cannot be greater than $T_1$ and the uncertainty principle predicts that the energy level is broadened by an amount

$$\frac{h}{T_1} \tag{7}$$

Now suppose we were to add an oscillating magnetic field with an energy equal to the difference of the two states of the nucleus. So:

$$h\nu = \Delta E = E_2 - E_1 \tag{8}$$

where $h$ is planck's constant, $\nu$ is the frequency of the magnetic field oscillations and $\Delta E$ is the energy difference between the two spin states. This oscillating field is used to stir up the nuclei so that the populations of these two energy states are equalized. This causes energy to be absorbed by the nuclei as they transition from the lower to the higher energy state and energy to be emitted as they transition back down to the lower state. By the addition of our oscillating field, we are repeatedly randomizing the distribution of nuclei

3 This is sort of the equivalent of ringing a bell once. The bell will ring (the nuclei align to the field) but nothing happens after that and the bell slowly stops producing a sound (the nuclei enter a Boltzmann distribution). As we're looking for resonance of a nuclei, we're going to need something to repeatedly stir up the nuclei after they've relaxed.

so that we can observe the frequency at which they change states. The major limitation here is that we want the nuclei to relax before we stir them up again, so we require

$$\frac{1}{\nu} \gg T_1 \tag{9}$$

The amount of energy being imparted to each nucleus by the oscillating field is small when compared to the energy from the static field so we can use time-dependent perturbation theory to describe the interaction. If *H* is the energy given by the static field, and *H′* is the energy given by the oscillating field then

$$H' = g\,\mu_N \vec{S}\cdot\vec{B} = h\,\nu \tag{10}$$

where *g* is the so-called g-factor, $\mu_N$ is the nuclear magneton[4], $\vec{S}$ is the spin of the nucleus, and $\vec{B}$ is the magnetic field vector. The g-factor can be solved for such that

$$g = \frac{h}{\mu_N}\cdot\frac{\nu}{|\vec{B}|} = \frac{\gamma\hbar}{\mu_N} \tag{11}$$

where $\gamma$ is the gyromagnetic ratio of the nucleus. The g-factor represents the ratio of the number of Bohr Magnetons to the units of $\hbar$ of angular momentum or to put it more simply, it is the point where the nucleus makes a transition from one spin state to another in units of MHz per Gauss and it is largely what we are attempting to find in our experiment.

The probability predicted for the transition from $E_2$ to $E_1$ (or the reverse) is given by Fermi's Golden Rule[5]

$$P = \frac{\Xi^2}{(\omega_o-\omega)^2+\Xi^2}\sin^2\left(\sqrt{(\omega_o-\omega)^2+\Xi^2}\right)\cdot\frac{t}{2} \tag{12}$$

where

$$\Xi = \frac{\omega_o H'}{H} \tag{13}$$

*t* is time, $\omega$ is the angular frequency induced from our oscillating field and $\omega_o$ is the Larmor frequency[6].

We now have a situation where the spins and magnetic moments are flipping up and down together with a certain frequency however, over time, the nuclei will not remain in sync with each other. Their transitions begin to become randomized such that, the cumulative effect is that there is no net change. That is, with randomized transitions, the number of nuclei making the upward transition is equal to the number of nuclei making a downward transition at any given time yielding a net change of zero. This is proven by using $N_1 - N_2 = 0$ in equation (6). This relaxation of the overall magnetization is the spin-spin relaxation time $T_2$ . In general, for a liquid, $T_1$ and $T_2$ tend to be equal, however for solids $T_1$ typically is larger than $T_2$.

After time $T_2$ the oscillations of the $\sin^2$ term in equation (12) are damped to an average of ½, yielding a transition probability of

$$P = \frac{\Xi^2}{(\omega_o-\omega)^2+\Xi^2}\cdot\frac{1}{2} \tag{14}$$

The change in the x, y, and z components of the magnetization with respect to time are related to $T_1$ and $T_2$ by the so-called Bloch equations[7].

4 See appendix for the value of $\mu_N$ and other constants.

5 See Griffiths, David J. *Introduction to Quantum Mechanics*. Upper Saddle River, NJ: Pearson Prentice Hall, 2005. Print. for more on this subject.

6 We see a resonance when $\omega = \omega_o$ .

7 Kittel, Charles. Introduction to Solid State Physics. New York: Wiley, 1996. Print.

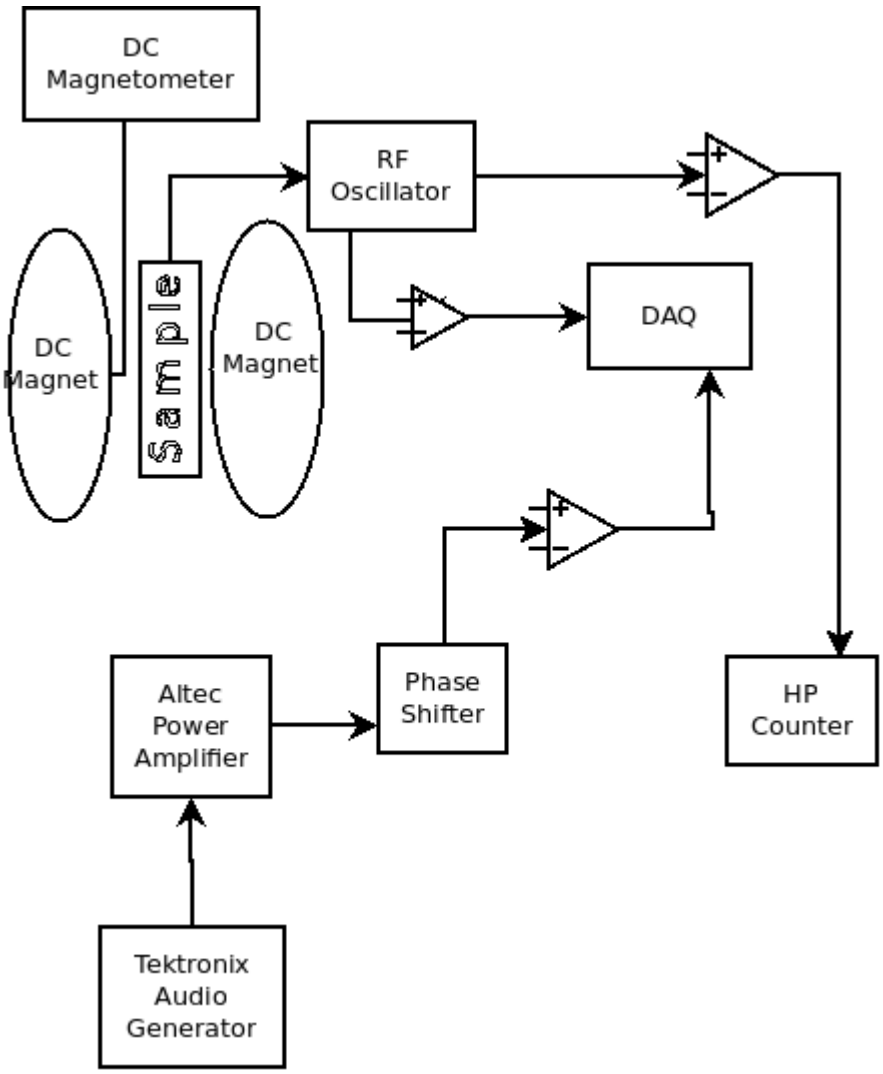


Figure 4: Our apparatus consisted of two large DC magnets (the source of our constant magnetic field) and a smaller coil was wrapped around the sample and provided the oscillating field. This oscillation was provided by an RF oscillator which also served as our sensor for detecting resonances. One output of the oscillator was sent to the HP Counter which gave a digital readout of the frequency of oscillations of the alternating field while a second output was sent to our data acquisition system (DAQ). We also had an audio generator's signal amplified and sent through a phase shifter before being sent to the DAQ. The audio signal allows us to sweep the magnetic field up and down slightly to give us a window where we can observe a resonance. As the signal sweeps back and forth across the oscilloscope, we use a phase shifter to adjust them so the two signals match up. In addition, we inserted a DC magnetometer next to the sample in order to measure the static magnetic field. The DAQ was used to take an average of the resonant waveform over the course of many resonances and output the waveform with as much noise as possible subtracted away.

$$\frac{dM_x(t)}{dt} = \gamma(\vec{M}(t)\times\vec{B}(t))_x - \frac{M_x(t)}{T_2} \quad (15)$$

$$\frac{dM_y(t)}{dt} = \gamma(\vec{M}(t)\times\vec{B}(t))_y - \frac{M_y(t)}{T_2} \quad (16)$$

$$\frac{dM_z(t)}{dt} = \gamma(\vec{M}(t)\times\vec{B}(t))_z - \frac{M_z(t)-M_o}{T_1} \quad (17)$$

where $\gamma$ is the gyro-magnetic ratio of the object and

$$\vec{B}(t) = B_o + \Delta B_z(t) \quad (18)$$

which is to say that the magnetic field overall is comprised of two components: the first from the static (DC) field and the second from the oscillating (AC) field which is changing with time.

In the Bloch equations, our magnetic fields are pointing in the $\hat{z}$ direction thus illustrating the axial symmetry implied by equations (15) and (16).

## EXPERIMENTAL PROCEDURE

The main goal of this experiment is to observe nuclear magnetic resonance in various substances. Specifically, we are measuring the resonances of the nuclei of Hydrogen[8], Florine, Lithium, Boron, and Phosphorus using substances which contain these elements as shown in table 1.

Our apparatus consisted of two large DC magnets (the source of our constant magnetic field) and a smaller coil near the sample to provide the oscillating field. This oscillation was provided by an RF oscillator which also served as our sensor for detecting a resonance.

| Nucleus | Sample(s) used | Approximate gyromagnetic ratio | Spin |
|---|---|---|---|
| $^{1}H$ | $H_2O$<br>$C_nH_{2n+2}$ | 42.5775 | 1/2 |
| $^{19}F$ | $C_6H_5CF_3$<br>$C_nF_{2n+2}$ | 40.0776 | 1/2 |
| $^{7}Li$ | $C_2H_3LiO_2$ | 16.5483 | 3/2 |
| $^{11}B$ | $HBF_4$ | 13.6630 | 3/2 |
| $^{31}P$ | $H_3PO_4$<br>$K_2HPO_4$ | 17.2515 | 1/2 |

Table 1: Shows the substances used to make measurements of the NMR properties of the nuclei of the listed elements. We used the given gyromagnetic ratios and spins to predict where we should see a resonance in order to prevent us from taking a measurement of a different nucleus. Approximate values taken from the CRC handbook or Chemistry and Physics, 86th Edition.

This RF oscillator is essentially an RLC circuit with the inductor wrapped around our sample. This circuit has a certain Q-factor or quality factor associated with it

$$Q = \frac{\omega L}{R} \quad (19)$$

and

$$\omega = 2\pi\nu \quad (20)$$

where $\nu$ is as defined in equation (8).

The oscillator actively polarizes the magnetic moments of the nuclei. The measure of how the field polarizes the nuclei is known as the magnetic susceptibility $\chi$ :

$$\chi = \frac{\vec{M}}{\vec{B}} \quad (21)$$

8 The Hydrogen nucleus is comprised only of a proton so we're essentially measuring the resonance of the proton itself.

This oscillator's coil is placed in the DC magnetic field at a 90 degree angle so that as the magnetization of the sample oscillates about the z-axis[9], the x and y components of this rotation induce a change in magnetic flux in the coil which can thus be measured.

One output of the oscillator was sent to the HP counter which gave a digital readout of the frequency of the alternating field while a second output was sent to our data acquisition system (DAQ). We also had an audio generator's signal amplified and sent through a phase shifter before being sent to the DAQ. The audio signal drives the DC magnetic field up and down slightly to give us a window where we can observe a resonance. That is, rather than trying to find a signal at an exact frequency and field strength, we vary the magnetic field slightly in order to take a snapshot of how the resonance behaves around a specific point As the signal sweeps back and forth across the oscilloscope, we use a phase shifter to adjust them so the two signals match up (see figures 13 - 17 for an example).

In addition, we inserted a DC magnetometer next to the sample in order to measure the DC magnetic field. The DAQ was used to take an average of the resonant NMR signal over 10,000 waveforms and output the the result with as much noise as possible subtracted away (see apparatus diagram in figure 4). The magnetic field measurements made by the DC magnetometer and the readout of the HP counter were inserted into equation (11) to find the g-factor and gyromagnetic ratio for that particular nucleus. In general, the magnetic fields we were using were on the order of a few thousand Gauss and the frequencies used were on the order of a few MHz.

The equipment used in our experiment is as follows:

- HP Universal Counter Model 5328A
- Varian DC Magnet
- Alphalab DC Magnetometer
- Altec Lansing Model 1268 Power Amplifier
- Tektronix Model SG-502 Oscillator
- A home-built phase shifter
- A home-built RF Oscillator
- 2 UC Davis Physics Model Amp-A Audio Buffer Amplifiers

The $T_2$ relaxation time could also be measured using the collected data. To measure $T_2$, we used our computer (DAQ) to average our NMR signal 10,000 times. We could then measure the full width at half max of the NMR signal's main dip as proportional to the relaxation time.

In general, we have some error associated with the data that we were recording. This error is based only on the perceived accuracy of the devices used to obtain our data points. The DC magnetometer that we were using to record the magnetic field tended to be stable only to about 1 Gauss and for this reason, all measurements taken with it are assumed to have an uncertainty of ± 1 Gauss. In addition, HP counter had an approximate uncertainty of about 1 KHz. This may be due to either a lack of stability in the RF Oscillator or the counter itself having trouble measuring the frequency. Either way, the error would manifest itself on the counter and thus all measurements taken with it have an uncertainty of ± 1 KHz.

## DATA ANALYSIS and RESULTS

In order to measure the g-factors of our samples, we graphed the points where we observed a resonance on a plot of magnetic field versus the radio frequency of our oscillator. We then took a least squares fit of the data and as indicated by equation (11), the slope is directly related to the gyromagnetic ratio. All of our data indicated a linear relationship between the radio

9 A reminder: the z-axis points in direction of the DC magnetic field.

| Nucleus | Measured gyromagnetic ratio (MHz/T) | Accepted gyromagnetic ratio (MHz/T) |
|---|---|---|
| $^{1}$H | 43.00 ± 0.01 | 42.5775 |
| $^{19}$F | 41.42 ± 0.01 | 40.0776 |
| $^{7}$Li | 16.1 ± 0.2 | 16.5483 |
| $^{11}$B | 13.66 ± 0.01 | 13.6630 |
| $^{31}$P | 17.30 ± 0.01 | 17.2515 |

Table 2: Table of measured gyromagnetic ratios as compared to accepted values taken from CRC Handbook of Chemistry and Physics, 86th edition. When 2 different values were obtained from our data (from multiple samples containing the same nucleus) the average is shown here.

frequency and the magnetic field strength, so a linear fit was used. All of the data sets had $\chi^2$ values which were very close to zero which indicates that the software package that we were using to perform our fit (Wavemetrics' IGOR) may have been performing some incorrect calculations with our error while creating a $\chi^2$ value for the fit line. The slope, however seems to be unaffected by this[10] and we still consider that measurement to be a good match to the data. These plots are shown in figures 5 through 12.

The slope values obtained were in units of MHz per Gauss and thus to compare to published values (given in units of MHz per Tesla) a conversion was required. The converted values and the current accepted published values of gyromagnetic ratios are shown in table 3.

In general, the gyromagnetic ratios that we measured were very close to published values. For example, our g-factor for Boron 11 is perhaps the strongest match to the published value with our result agreeing as far as the accuracy of our measurement allows. Aside from the Boron sample, our measurement of Phosphorus resonance was also in close proximity to the CRC's value. While our error bars don't quite include the CRC value, we are still quite close.

For the remaining three samples (Fluorine, Lithium, and Hydrogen) our measurements differ slightly from the CRC values, however, they are still within 1.5 MHz per Tesla at the largest deviation. Our measurements all tend to agree very closely with the majority of other published values.

From the gyromagnetic ratio, it is also possible to calculate the g-factor of the nucleus as shown in equation (11). The gyromagnetic ratios only differ from the g-factor by a constant factor of $\frac{h \cdot 10^6}{\mu_N}$ [11] and their direct calculation merely serves to further validate our measurements. The g-factors calculated matched published values by the same relative amount of the gyromagnetic ratios further implying a good agreement(shown in table 3).

| Nucleus | Measured g-factor | Accepted g-factor |
|---|---|---|
| $^{1}$H | 5.637 ± 0.001 | 5.5814 |
| $^{19}$F | 5.4297 ± 0.0001 | 5.2537 |
| $^{7}$Li | 2.11 ± 0.02 | 2.1693 |
| $^{11}$B | 1.791 ± 0.001 | 1.7911 |
| $^{31}$P | 2.268 ± 0.001 | 2.2615 |

Table 3: Table of measured g-factors as compared to accepted values taken from CRC Handbook of Chemistry and Physics, 86th edition. All values were calculated using equation (11) and table 2.

The final measurement that we took was of the $T_2$ relaxation times of the samples. The plots shown in figures 13 through 17 are of the power absorption of the nucleus with respect to magnetic

10 In fact, the slope calculated by the fit is very close to the slope that is calculated by taking the lowest and highest points of our data. As our data appears to be highly linear in nature, we can accept the least squares slope as accurate with a reasonable degree of confidence.

11 The factor of $10^6$ comes from converting our frequency from MHz to Hz.

| Nucleus | Measured $T_2$ (seconds) |
|---|---|
| $^{1}H$ | 0.005 |
| $^{19}F$ | 0.010 |
| $^{7}Li$ | 0.015 |
| $^{11}B$ | 0.015 |
| $^{31}P$ | 0.013 |

Table 4: Table of approximate $T_2$ relaxation times as indicated by our data. No errors are given as the numerical error in calculation is obviously overshadowed by a more prevalent systematic error. This systematic error is indicated by the proximity of the relaxation times to each other.

field fluctuations. As the x-axis is given in units of Gauss, we were required to attain a calibration factor to see how time was changing with respect to the magnetic field fluctuations. The relationship used was

$$\Delta \nu = \gamma \Delta B \tag{22}$$

where $\Delta B$ is the full width at half max of the main dip in the NMR curve, $\gamma$ is the gyromagnetic ratio of the nucleus as given in table 2, and $\Delta \nu$ is the corresponding difference in frequency required for relaxation to occur. We could therefore take

$$T_2 \approx \frac{1}{\Delta \nu} \tag{23}$$

These relaxation times, although an approximation, tend to be grouped quite closely. As published values were not available, it is difficult to ascertain how our calculations compare, however we can speculate on this effect. As the spin-spin relaxation time has to do with the motions of the nuclei in a medium, you would expect the time to be related in some manner to the gyromagnetic ratio of the nucleus. Seeing as how our ratios exhibit a significant spread in value, we would expect this spread to propagate in some fashion to the relaxation times and we can therefore expect them to exhibit a similar distribution.

The cause of this apparent error is likely to be due to inhomogeneities in our magnetic field. If the magnetic field is fluctuating randomly about the resonant value, as our DAQ took the average of the waveform over many cycles, it would cause the waveform to smear or broaden in the x direction by the approximate amount of the fluctuations[12] which would thus place a minimum width that we can detect on our NMR signal. Given this fact, it would appear that the true relaxation times of our samples are beyond the resolution available from our equipment.

## DISCUSSION

Our results for the gyromagnetic ratio and g-factor (along their proximity to other published values) are a good indication that the experiment had a very low susceptibility to random errors. In fact, the main source of error for this experiment appears to be purely systematic in that generally our measurements of gyromagnetic ratios tended to be larger than the CRC Handbook's values.

While our estimates of the relaxation times of the nuclei were most likely incorrect, it was not at the fault of the methodology, but merely an unaccounted for source of systematic error which limited our resolution. Our measurements of $T_2$ are still useful in one respect: they place a maximum value on the full width at half max of the NMR signals. Further measurements of this effect should expect to see a width less than what we have observed.

This obstacle could easily be overcome through the use of an electromagnet with a more stable power supply. In addition, our apparatus was located near a second electromagnet which, while not powered, likely still exhibits a magnetic

12 Recall that the x-axis of the absorption curve is the magnetic field.

field which could affect our experiment. In fact, with our electromagnet powered off, the Gauss meter registered approximately 80 Gauss in the region of our sample implying an external field may have been having a slight affect on our measurements. This could easily the remedied through the use of shielding, or a more accurate measurement of the background magnetic field's strength.

Other factors affecting our measurements include random errors associated with the placement of the sample in the magnetic field which could be reduced through the use of a restraint to hold the oscillator coil in the same place as the samples are changed.

Perhaps our largest source of error stems from a low signal-to-noise ratio for most of the NMR signals observed. While the averages calculated for the relaxation times can be trusted (aside from the field inhomogeneity) the low signal-to-noise ratio often made it difficult to pin down the exact magnetic field strength of the resonance. This can be improved through the use of the DAQ to average the signals over many waveforms, however this comes at the cost of a dramatic increase in the time required for the experiment.

In addition, we were using two different probes to take the measurements. One probe was sensitive to radio frequencies less that ~11 MHz and the other probe was sensitive frequencies greater than ~11 MHz. This is an obvious source of error as it is unlikely that these different probes have the same degree of accuracy. Also, whenever we changed the probes, we were required to remove the sample from the magnet, thus changing it's position when we re-inserted it to to field to continue taking measurements. This change in the data is perhaps most apparent in measurement of fluorine in figure 7. Much of the data below ~10 MHz is below the fit line while much of the data above ~12 MHz is above the fit line. This effect is an unknown source of error and could be accounted for by taking data with the two probes separately, fitting the data separately, and seeing how the two values differ.

As a higher degree of accuracy is attained, and the number of different samples tested is increased, these measurements will further aid in the detection of elements in chemical samples for other scientific experiments as well as help with the diagnosis of medical maladies through the use of magnetic resonance imaging (MRI) scans.

All factors considered, this experiment can be deemed a success. The gyromagnetic ratios and g-factors of the various nuclei are in close agreement with the accepted values in the scientific community and indicate that this apparatus has a high degree of accuracy and precision for this sort of measurement. Overall, the results confirm that we are in fact observing nuclear magnetic resonance which conforms to the accepted theory closely.

## CONCLUSION

The purpose of this experiment was to accurately measure the gyromagnetic ratio and g-factor of the Hydrogen, Fluorine, Lithium, Boron, and Phosphorus nuclei. The final values attained are shown below.

| Nucleus | Measured gyromagnetic ratio (MHz/T) | Measured g-factor |
|---|---|---|
| $^{1}H$ | 43.00 ± 0.01 | 5.637 ± 0.001 |
| $^{19}F$ | 41.42 ± 0.01 | 5.4297 ± 0.0001 |
| $^{7}Li$ | 16.1 ± 0.2 | 2.11 ± 0.02 |
| $^{11}B$ | 13.66 ± 0.01 | 1.791 ± 0.001 |
| $^{31}P$ | 17.30 ± 0.01 | 2.268 ± 0.001 |

We were able to attain a high level of accuracy with measurements that conform quite closely to published values in the CRC handbook. Our estimations of the $T_2$ relaxation times of these nuclei suffered from a limitation by systematic error, however the estimates still provide a

maximum value for the width of a resonant signal and can thus be used to check the results of further experimentation.

## Acknowledgments

I would like to acknowledge the help of Alex Shei and Valentina Prelipina. Without their insights into the apparatus and theory of this experiment, I would still be making measurements of a signal that didn't exist. In addition, Professor Xiangdong Zhu and Sergey Uvarav proved instrumental in my understanding of the observed effects and errors. Their help is greatly appreciated.

# Appendix/Figures

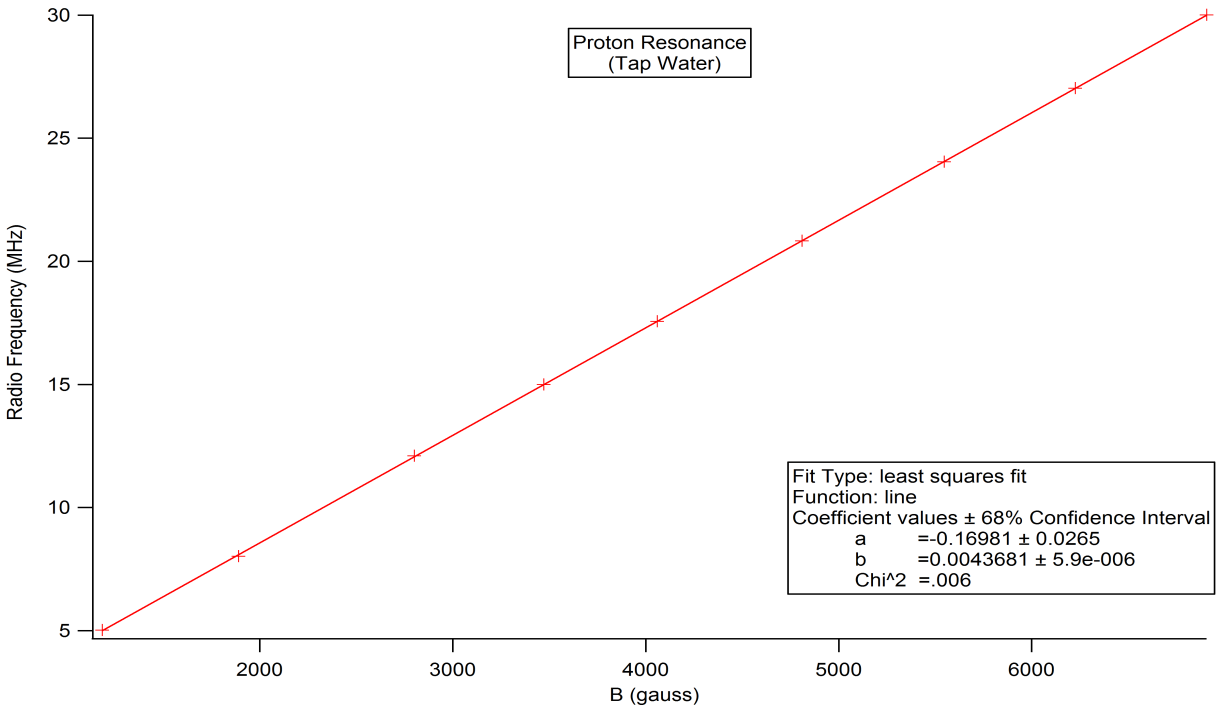


Figure 5: A plot of radio frequencies vs. magnetic field values of Proton resonance from a tap water sample. The data is fitted with a least squares linear fit where the slope is the gyromagnetic ratio. The measurement of $\gamma$ here is 0.004368 ± 0.000006 MHz per Gauss.

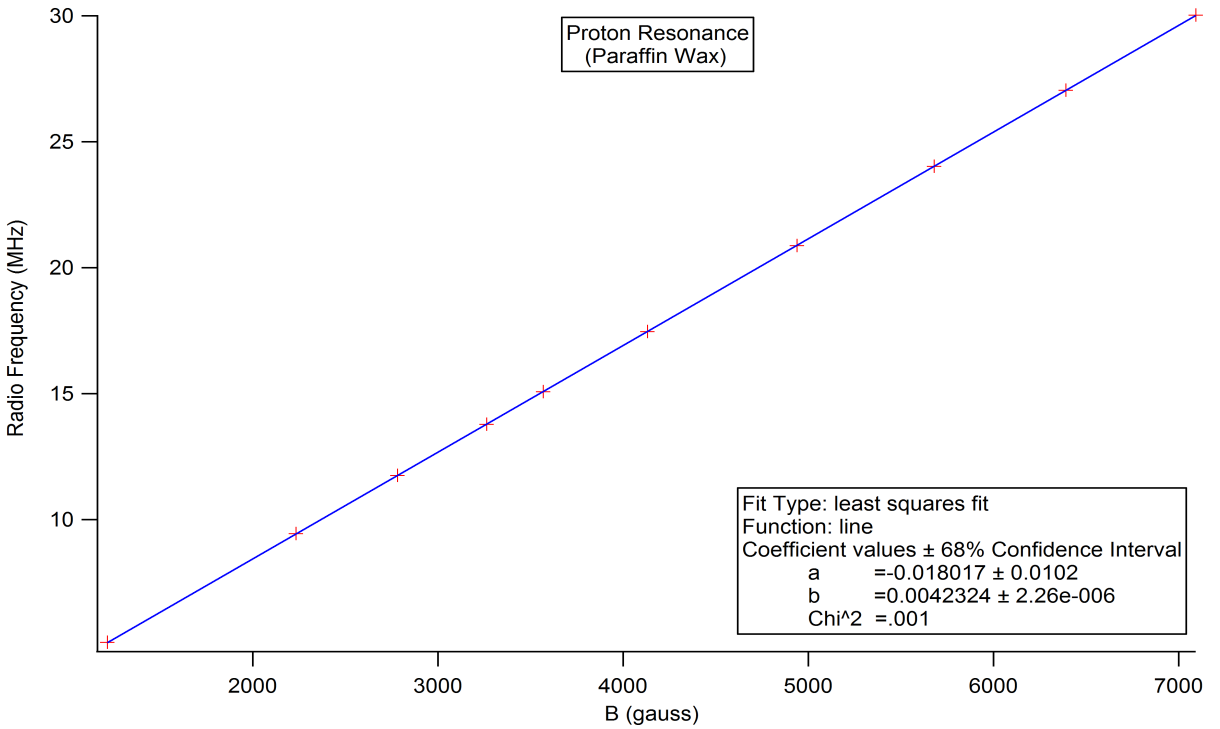


Figure 6: A plot of radio frequencies vs. magnetic field values of Proton resonance from a $C_nH_{2n+2}$ sample. The data is fitted with a least squares linear fit where the slope is the gyromagnetic ratio. The measurement of $\gamma$ here is 0.004232 ± 0.000002 MHz per Gauss.

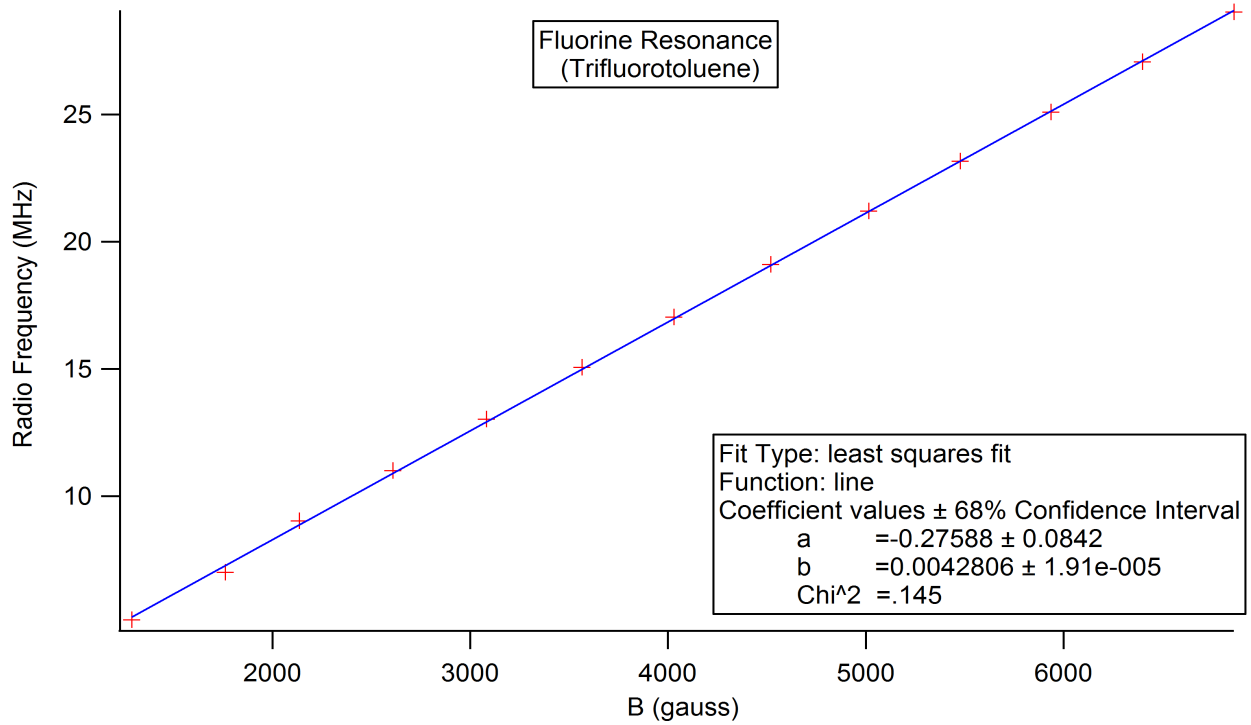


Figure 7: A plot of radio frequencies vs. magnetic field values of Fluorine resonance from a $C_6H_5CF_3$ sample. The data is fitted with a least squares linear fit where the slope is the gyromagnetic ratio. The measurement of $\gamma$ here is 0.00428 ± 0.00002 MHz per Gauss.

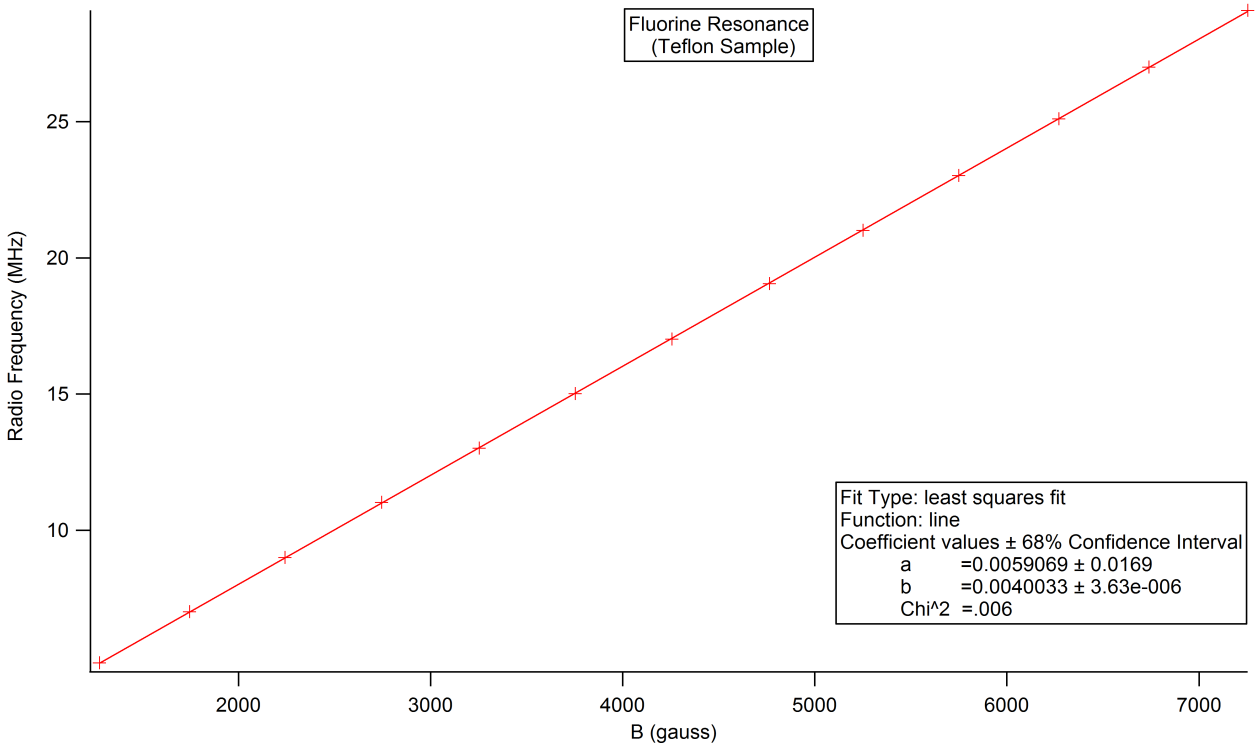


Figure 8: A plot of radio frequencies vs. magnetic field values of Fluorine resonance from a $C_nF_{2n+2}$ sample. The data is fitted with a least squares linear fit where the slope is the gyromagnetic ratio. The measurement of $\gamma$ here is 0.004003± 0.000004 MHz per Gauss.

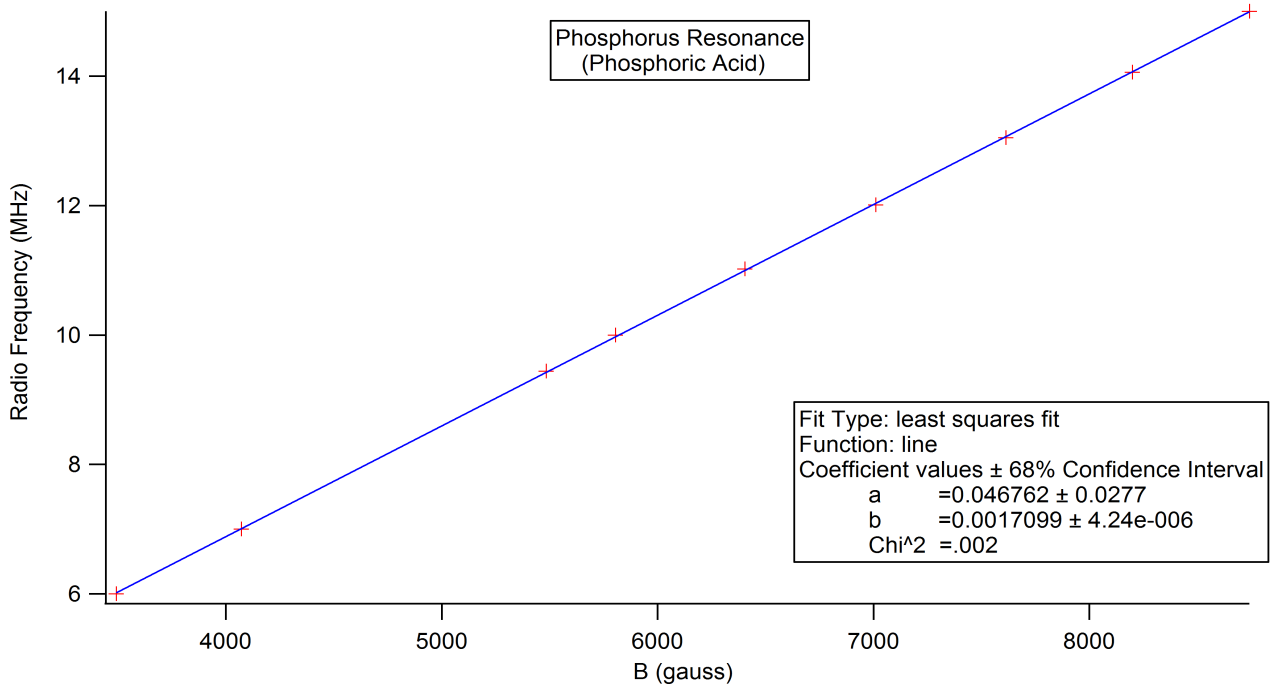


Figure 9: A plot of radio frequencies vs. magnetic field values of Phosphorus resonance from a $H_3PO_4$ sample. The data is fitted with a least squares linear fit where the slope is the gyromagnetic ratio. The measurement of $\gamma$ here is 0.001710 ± 0.000004 MHz per Gauss.

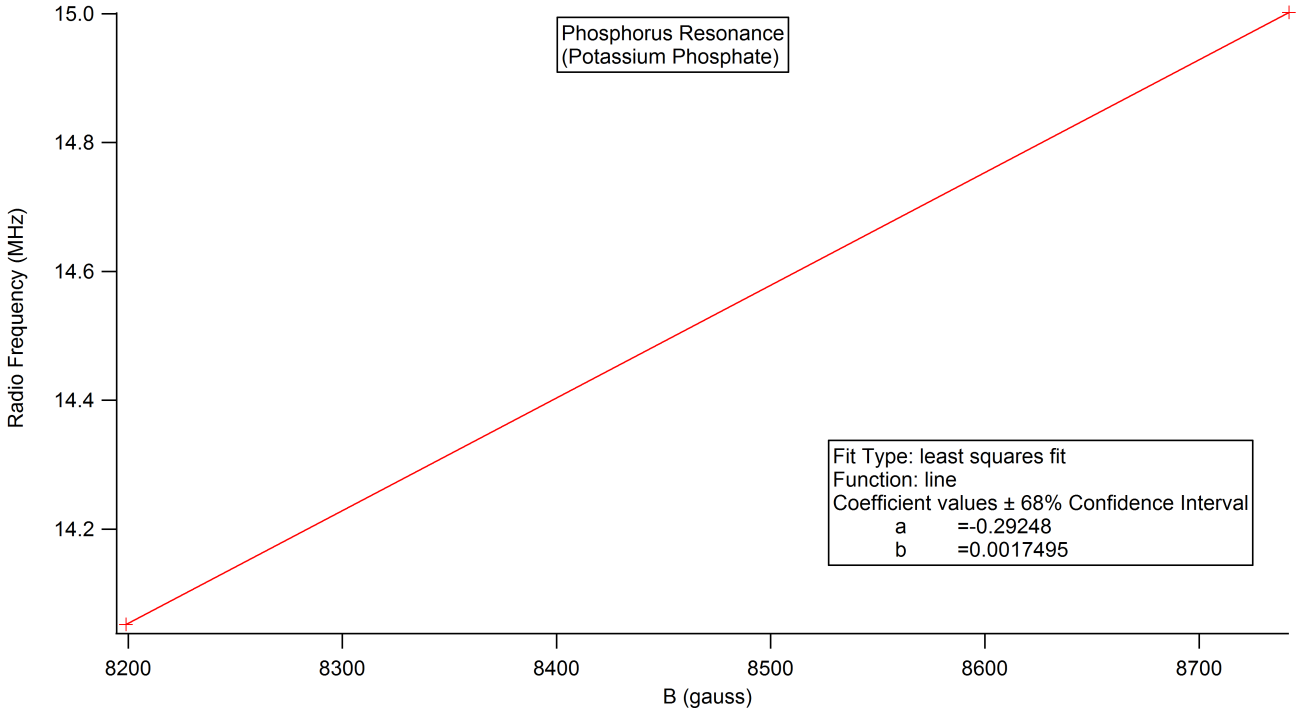


Figure 10: A plot of radio frequencies vs. magnetic field values of Phosphorus resonance from a $K_2HPO_4$ sample. The data is fitted with a least squares linear fit where the slope is the gyromagnetic ratio. The measurement of $\gamma$ here is 0.0017495 MHz per Gauss. There is no reduced $\chi^2$ value as this slope is achieved from a line drawn between the only two data points we could achieve due to an extremely poor signal to noise ratio.

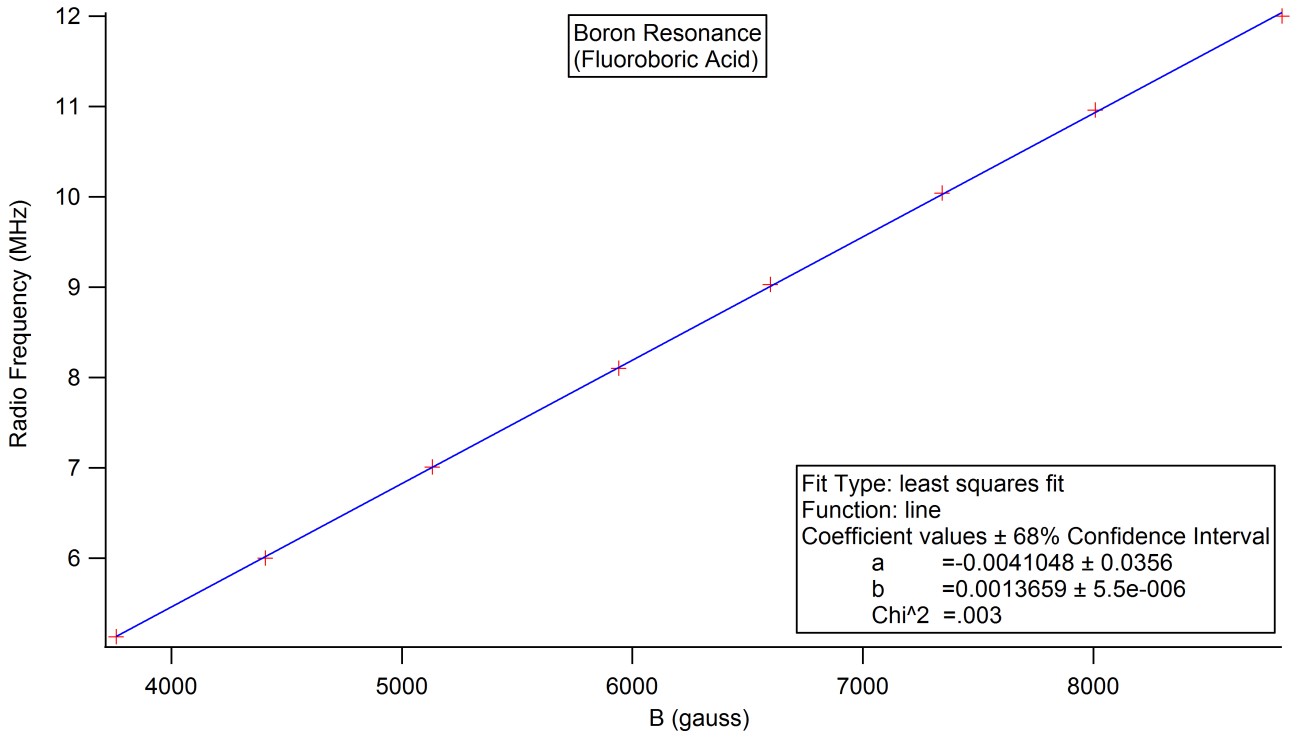


Figure 11: A plot of radio frequencies vs. magnetic field values of Boron resonance from a $HBF_4$ sample. The data is fitted with a least squares linear fit where the slope is the gyromagnetic ratio. The measurement of $\gamma$ here is 0.001366 ± 0.000006 MHz per Gauss.

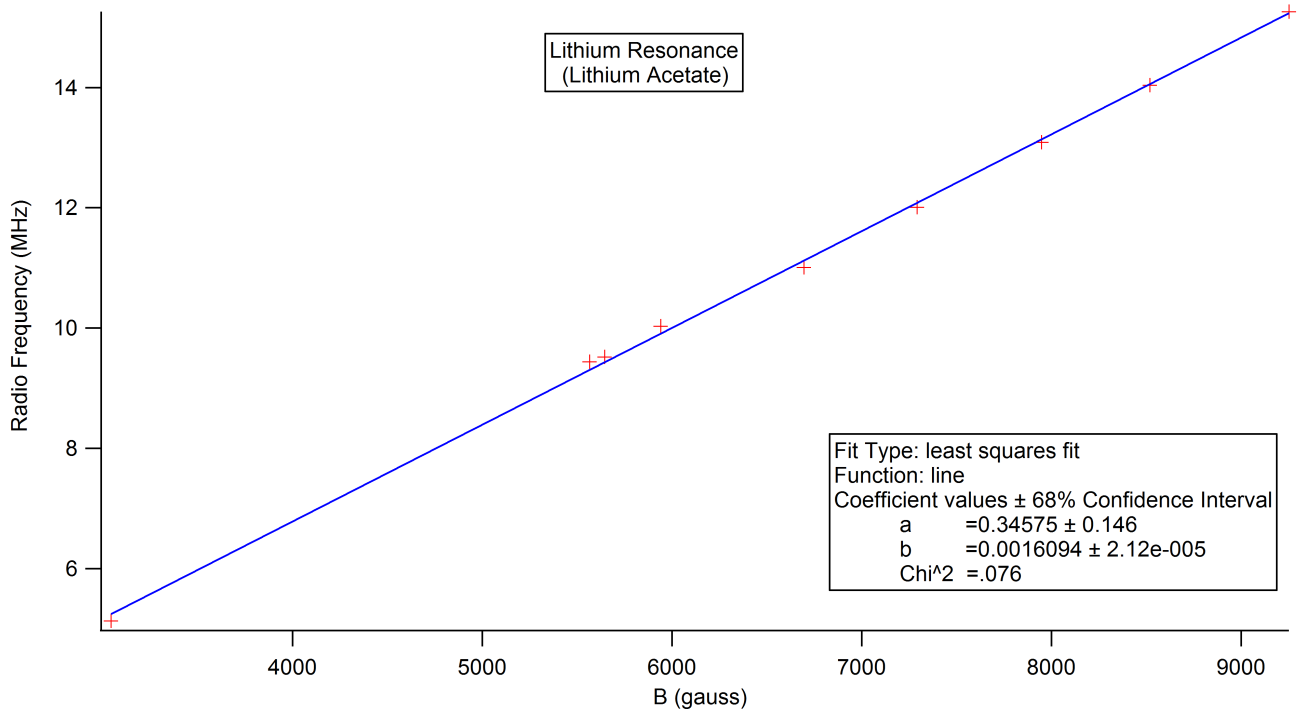


Figure 12: A plot of radio frequencies vs. magnetic field values of Lithium resonance from a $C_2H_3LiO_2$ sample. The data is fitted with a least squares linear fit where the slope is the gyromagnetic ratio. The measurement of $\gamma$ here is 0.00161 ± 0.00002 MHz per Gauss.

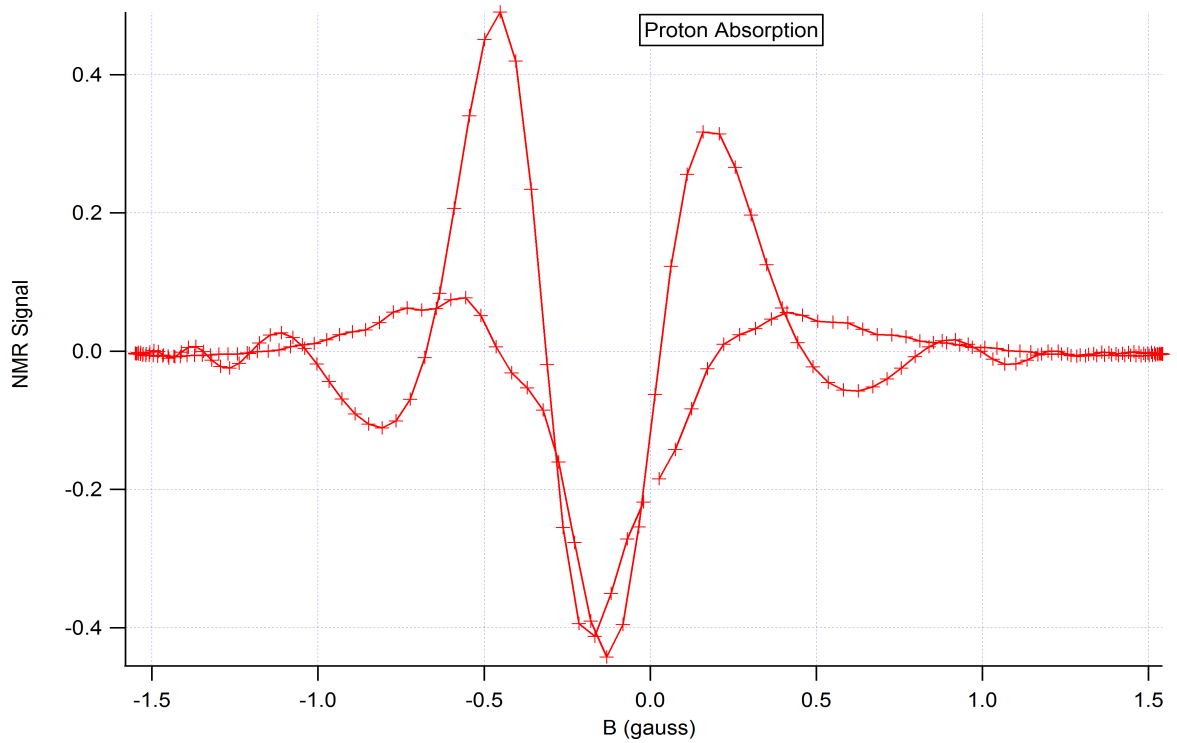


Figure 13: A plot of the NMR signal against the magnetic field fluctuations for the proton resonance. The full width at half max of the main dip (approx 0.45 Gauss) is used in the calculation of the spin-spin relaxation time.

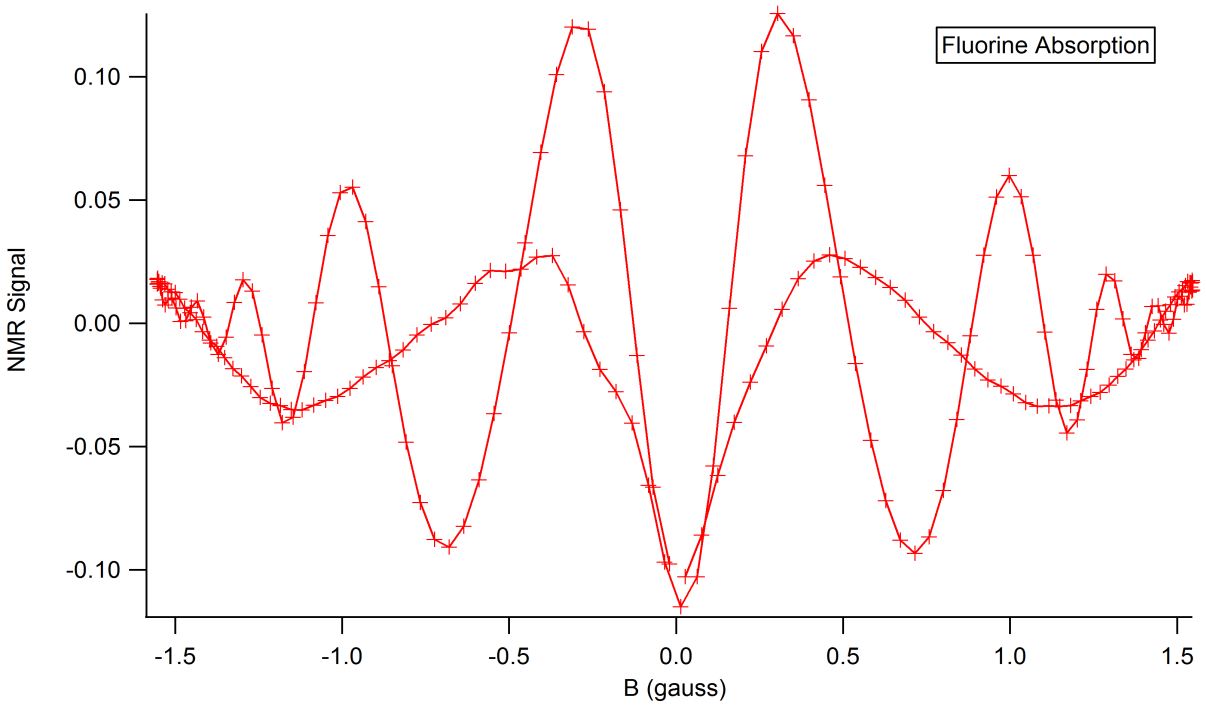


Figure 14: A plot of the NMR signal against the magnetic field fluctuations for the Fluorine nuclear resonance. The full width at half max of the main dip (approx 0.25 Gauss) is used in the calculation of the spin-spin relaxation time.

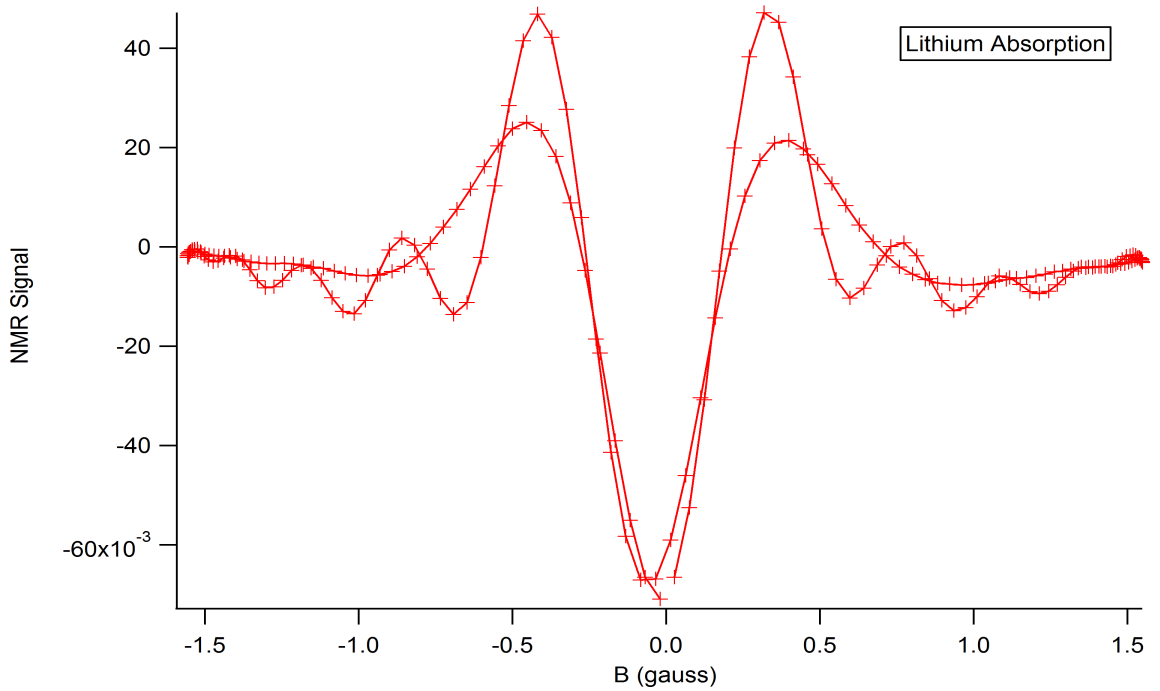


Figure 15: A plot of the NMR signal against the magnetic field fluctuations for the Lithium nuclear resonance. The full width at half max of the main dip (approx 0.4gauss) is used in the calculation of the spin-spin relaxation time.

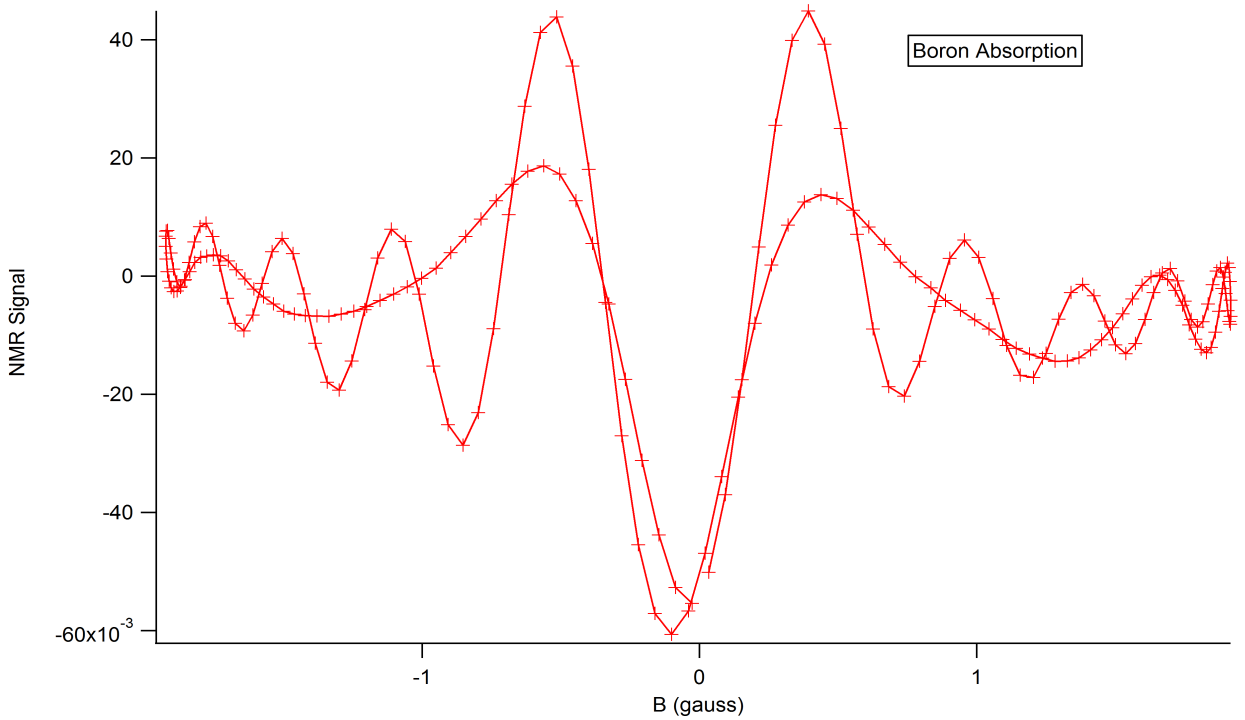


Figure 16: A plot of the NMR signal against the magnetic field fluctuations for the Boron nuclear resonance. The full width at half max of the main dip (approx 0.5 Gauss) is used in the calculation of the spin-spin relaxation time.

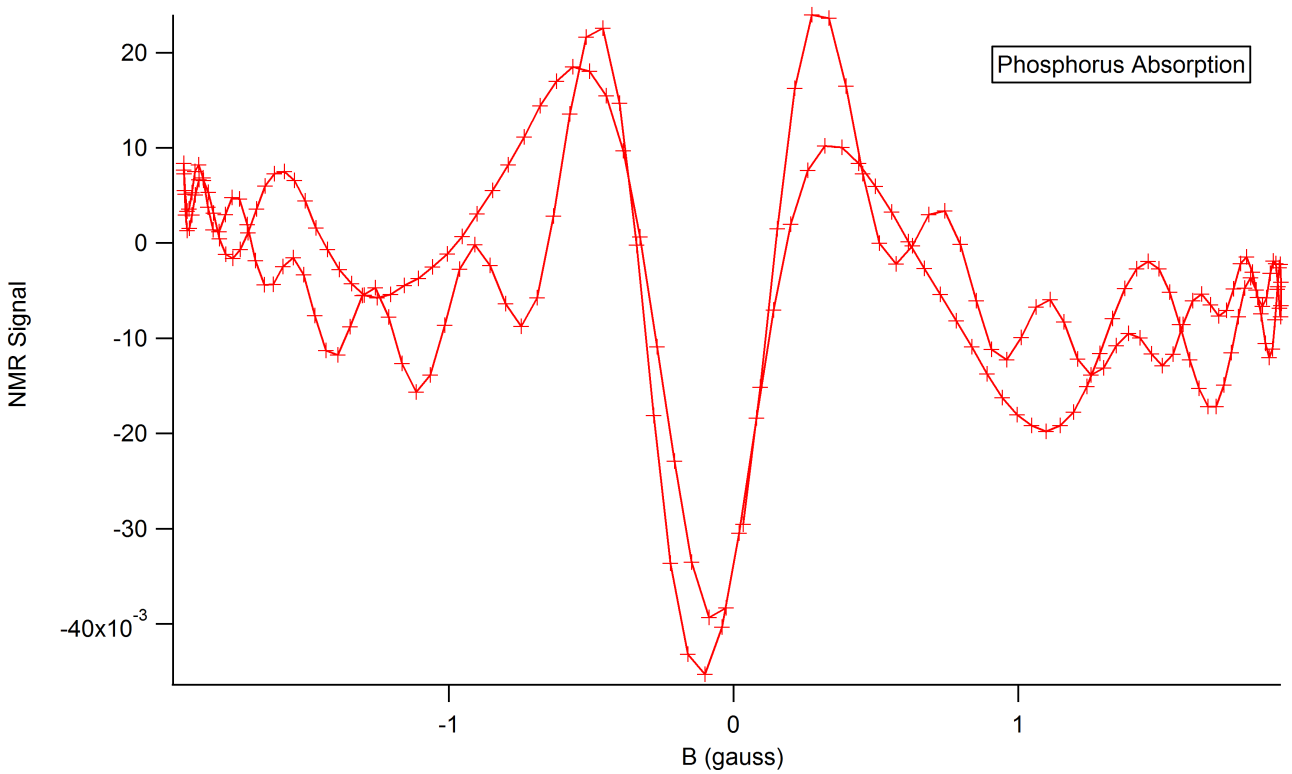

Figure 17: A plot of the NMR signal against the magnetic field fluctuations for the Phosphorus nuclear resonance. The full width at half max of the main dip (approx 0.45 Gauss) is used in the calculation of the spin-spin relaxation time.

Constants used:

$$\mu_N = \frac{e\hbar}{2mc} = 5.05078234 \times 10^{-31} \frac{J}{G}$$

$$e = 1.60217646 \times 10^{-19}\, C$$

$$\hbar = 1.05457148 \times 10^{-34} \frac{m^2\, kg}{s}$$

$$m_p = 1.67262158 \times 10^{-27}\, kg$$

References by footnote:

5) Griffiths, David J. *Introduction to Quantum Mechanics*. Upper Saddle River, NJ: Pearson Prentice Hall, 2005. Print.

7) Kittel, Charles. Introduction to Solid State Physics. New York: Wiley, 1996. Print.

Other data as cited, taken from:

Lide, David R. CRC Handbook of Chemistry and Physics: a Ready-reference Book of Chemical and Physical Data. Boca Raton, Fla.: CRC Taylor & Francis, 2006. Print.